MOLECULAR AND CELLULAR BIOLOGY, Apr. 2008, p. 2590–2597 Vol. 28, No. 8
0270-7306/08/$08.00+0 doi:10.1128/MCB.01889-07

Rgs5 Targeting Leads to Chronic Low Blood Pressure and a Lean Body Habitus▽

Hyeseon Cho,[1]* Chung Park,[1] Il-Young Hwang,[1] Sang-Bae Han,[2] Dan Schimel,[3] Daryl Despres,[3] and John H. Kehrl[1]*

B-Cell Molecular Immunology Section, Laboratory of Immunoregulation, National Institute of Allergy and Infectious Diseases,[1] and Mouse Imaging Facility, National Institute of Neurological Disorders and Stroke,[3] National Institutes of Health, Bethesda, Maryland 20892-1876, and College of Pharmacy, Chungbuk National University, Cheongju, Republic of Korea[2]

Received 18 October 2007/Returned for modification 7 December 2007/Accepted 29 January 2008

RGS5 is a potent GTPase-activating protein for $G_{i\alpha}$ and $G_{q\alpha}$ that is expressed strongly in pericytes and is present in vascular smooth muscle cells. To study the role of RGS5 in blood vessel physiology, we generated *Rgs5*-deficient mice. The *Rgs5*$^{-/-}$ mice developed normally, without obvious defects in cardiovascular development or function. Surprisingly, *Rgs5*$^{-/-}$ mice had persistently low blood pressure, lower in female mice than in male mice, without concomitant cardiac dysfunction, and a lean body habitus. The examination of the major blood vessels revealed that the aortas of *Rgs5*$^{-/-}$ mice were dilated compared to those of control mice, without altered wall thickness. Isolated aortic smooth muscle cells from the *Rgs5*$^{-/-}$ mice exhibited exaggerated levels of phosphorylation of vasodilator-stimulated phosphoprotein and extracellular signal-regulated kinase in response to stimulation with either sodium nitroprusside or sphingosine 1-phosphate. The results of this study, along with those of previous studies demonstrating that RGS5 stability is under the control of nitric oxide via the N-end rule pathway, suggest that RGS5 may balance vascular tone by attenuating vasodilatory signaling in vivo in opposition to RGS2, another RGS (regulator of G protein signaling) family member known to inhibit G protein-coupled receptor-mediated vasoconstrictor signaling. Blocking the function or the expression of RGS5 may provide an alternative approach to treat hypertension.

The maintenance of normal blood pressure (BP) is achieved in part by balancing the constriction and dilatation of resistance arterioles via vasoregulatory G protein-coupled receptors (GPCRs). When activated by ligand binding, these GPCRs function as guanine nucleotide exchange factors for heterotrimeric G proteins, triggering downstream effectors and thus producing the biological responses attributed to these receptors. The GTPase activity of G_α subunits is subject to control by GTPase-activating proteins (GAPs) called regulators of G protein signaling (RGS) proteins. RGS proteins limit the duration that G_α subunits remain GTP bound, thereby negatively regulating GPCR-mediated signaling pathways. Numerous studies with genetically modified animals and with genetic polymorphisms of human populations have underscored the importance of GPCR agonists, GPCRs, and components of GPCR-mediated signaling pathways in BP homeostasis (for a review, see reference 24).

A member of the RGS family, RGS2, and GPCR kinase 2 (GRK2), GRK4, and GRK5 have been implicated previously in the regulation of BP. RGS2 is a potent negative regulator of $G_{q\alpha}$, and mice lacking RGS2 are hypertensive due to prolonged signaling by vasoconstrictor GPCR signaling pathways involved in BP control (12). The overexpression of GRK2 or GRK5 in vascular smooth muscle cells (VSMC) also results in a hypertensive phenotype by decreasing GPCR-mediated vasodilation and simultaneously enhancing GPCR-mediated vasoconstriction (8, 15). A defective coupling between the dopamine receptor and the G protein-effector complex as a result of mutation in GRK4 is reported to be the cause of the impaired renal dopaminergic action in genetic rodent and human essential hypertension (for a review, see reference 9).

RGS5, a member of the RGS family, exhibits a striking expression pattern in VSMC/pericytes and is a potent GAP for $G_{i\alpha}$ and $G_{q\alpha}$, suggesting a role in BP regulation (5, 7). Recent genome-wide linkage and candidate gene-based association studies have identified the human *Rgs5* gene as one of the three genes that contribute to elevated BP in the population at large (6). To determine whether RGS5 is required for normal BP homeostasis, we have generated and analyzed mice lacking a functional *Rgs5* gene. Here we report that *Rgs5*$^{-/-}$ mice are hypotensive, without any apparent anatomical defects or cardiac dysfunction. Our physiological and signaling analyses of these mutant mice, in addition to previously published results, suggest that the fine-tuning of both GPCR-mediated vasoconstrictor and vasodilatory signaling by RGS proteins is required for normal BP homeostasis.

MATERIALS AND METHODS

Generation of *Rgs5*$^{-/-}$ mutant mice. The targeting construct was designed by replacing parts of exon 1 and intron 1 of the *Rgs5* gene with a dual cassette containing the *lacZ* and neomycin resistance genes. Ten micrograms of the linearized targeting construct was introduced by electroporation into 129Sv/Ev embryonic stem cells to generate targeted embryonic stem cell clones. After selection with G418, surviving colonies were expanded and PCR analysis was performed to identify clones that had undergone homologous recombination.

* Corresponding author. Mailing address: Laboratory of Immunoregulation, National Institute of Allergy and Infectious Diseases, National Institutes of Health, Bldg. 10, Room 11B08, 10 Center Dr. MSC 1876, Bethesda, MD 20892. Phone for Hyeseon Cho: (301) 496-6363. Fax: (301) 402-0070. E-mail: hcho@niaid.nih.gov. Phone for John H. Kehrl: (301) 443-6907. Fax: (301) 402-0070. E-mail: jkehrl@niaid.nih.gov.

▽ Published ahead of print on 11 February 2008.

The identified positive clone was injected into C57BL/6 blastocysts. Chimeric mice were bred, and germ line transmission was confirmed (data not shown). Genotypes were further determined by PCR analyses of genomic DNA isolated from tails using *Rgs5*-specific primers. Mice were housed under specific-pathogen-free conditions and used in accordance with the guidelines of the Institutional Animal Care Committee at the National Institutes of Health.

RNA isolation and RT-PCR analysis. Harvested mouse tissues were frozen with liquid nitrogen and ground using a mortar and pestle. Total RNA was isolated from the ground tissues by using an RNA kit (Qiagen, Valencia, CA) with DNase treatment. The cDNA was generated using an Advantage reverse transcription (RT)-for-PCR kit (Clontech, Palo Alto, CA). PCR was performed with cDNA using HotStarTaq master mix (Qiagen). The following primer pairs specific for mouse *Rgs* and *Gna* genes were used to monitor mRNA expression: *Rgs2*, AGTGCAGGCAACGGCCCCAAG (forward) and TGGGGCTCCGTG GTGATCTGT (reverse); *Rgs4*, GCCGGCTTCCTGCCTGAGGAG (forward) and ACCAGGGAAGTGCAGTCTGCA (reverse); *Rgs5*, ATGTGTAAGGGA CTGGCAGCTCTGCCGCAC (forward) and CTTGATTAGCTCCTTATAAA ATTCAGAGCG (reverse); *Rgs16*, CAGAGCTGAGCTCCGATACTGGGG (forward) and GGGTGCAGAGGTGGAAGTGGCCGA (reverse); *Gnai1*, GA CTTCGGAGACTCTGCTCGG (forward) and ACTGTCTTTCCACAGTCT CTTT (reverse); *Gnai2*, GACTTTGCTGATCCCCAG (forward) and GTCAC TCTGTGCAATGCGC (reverse); *Gnai3*, GGGGAGAAAGCGGCCAAA (forward) and CTCCCAGCTAAAACAAATAAC (reverse); *Gnaq*, AAGCCC GGAGGATCAACGAC (forward) and CGCGCTTGTCTTCGTCAGAGT (reverse); and *Gnas*, GGGCTGCCTCGGCAACAG (forward) and GCGTGGCC CGGTAGACCTGC (reverse). A mouse β-actin primer pair was used for the normalization of cDNA synthesis.

BP analysis. Tail BPs of awake mice were recorded by using a computer-automated tail cuff MC-4000 BP analysis system (Hatteras Instruments, Cary, NC). Mice were first acclimated on the machine for 2 days, and to average out some day-to-day variation, BP was measured in the morning for 3 days. The mice were contained in individual dark chambers on a preheated platform to increase blood flow to the tail, and their tails were threaded through a tail cuff. Once contained in a measurement chamber, each mouse underwent 10 preliminary cycles, for which data were not recorded. The actual measurement of tail arterial pressure (in millimeters of mercury) was then performed until 20 measurement cycles were completed. A given mouse had to have a minimum of 15 successful measurement cycles out of 20 cycles for the data to be accepted. The reported data are mean values obtained from three to five mice and were analyzed for statistical significance by Student's *t* test.

Echocardiography, electrocardiography, and computer tomography (CT). Mice were anesthetized by the inhalation of 1 to 2% isoflurane delivered in a gas mixture with oxygen, medical-grade compressed air, and nitrogen. The Vevo 770 microultrasound system (VisualSonics Inc., Toronto, Canada) was used for echocardiography with anesthetized mice. The left ventricles were assessed in both parasternal long-axis and short-axis views at a frame rate of 60 Hz with a 40-MHz transducer. Data were captured in B mode, M mode, and Doppler mode. Electrocardiography was performed with conscious mice by using the ECGenie electrocardiography system (Mouse Specifics, Inc., Boston, MA). Only data from continuous recordings of 20 to 30 electrocardiography signals were used in the final analyses. Data were analyzed by using eMOUSE, a physiologic waveform analysis platform (Mouse Specifics, Inc.). The reported data are mean values obtained from three to five mice and were analyzed for statistical significance by Student's *t* test.

CT scan images were acquired using an X-ray micro-CT imaging system with anesthetized mice. To obtain three-dimensional volumetric data, full 360-degree scans were performed at 1/2-degree steps (720 projections). Mice in the scanner were monitored by direct observation or by observation on a video monitor. Body temperature was maintained by warming inspired anesthetic gases and disposable hand warmers. An iodinated contrast agent, Fenestra-VC (Advanced Research Technologies, Montreal, Canada), was intravenously administered at a dose of 0.0175 ml per g of body weight approximately 3 h prior to scanning. Images were reconstructed and analyzed using Amira 4.1 (Mercury Computer Systems, Inc., Chelmsford, MA).

Histology and morphometric analysis of vasculature. Mice were perfused at constant pressure with 10% phosphate-buffered formalin. Sections of paraffin-embedded tissues were prepared and stained with Verhoeff-Van Gieson (VGE) reagent for elastin staining or with hematoxylin and eosin. Images of aorta and kidney vessels were acquired using Image-Pro (Media Cybernetics, Silver Spring, MD). Morphometric analysis was performed using the measurement module of Image-Pro. The reported data are mean values obtained from four mice and were analyzed for statistical significance by Student's *t* test.

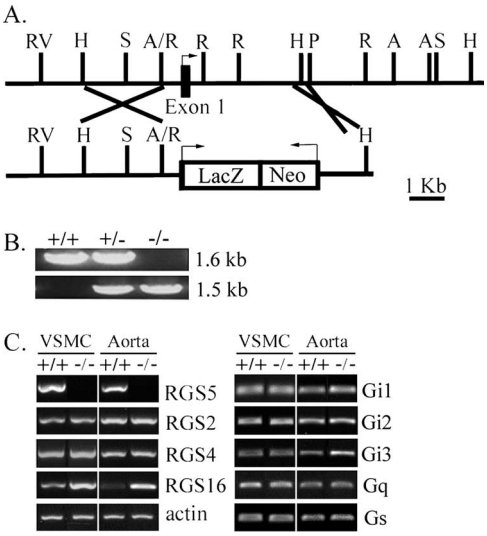

FIG. 1. Generation of *Rgs5*-targeted mice. (A) Schematic of *Rgs5* targeting construct to generate RGS5-deficient mice. Parts of exon 1 and intron 1 of the mouse *Rgs5* gene were replaced with a cassette comprising the *lacZ* gene and a neomycin resistance marker (Neo). Arrows indicate the direction of transcription. Restriction enzymes: A, AvrII; H, HindIII; P, PacI; R, EcoRI; RV, EcoRV; and S, SmaI. (B) PCR analysis of genomic DNA from $Rgs5^{+/+}$ (+/+), $Rgs5^{+/-}$ (+/−), and $Rgs5^{-/-}$ (−/−) mice to verify *Rgs5* gene targeting. The PCR product from wild-type genomic DNA is 1.6 kb, while the product generated from RGS5-deficient mice is 1.5 kb. (C) RT-PCR analysis to assess the expression of *Rgs2*, *Rgs4*, *Rgs5*, *Rgs16*, *Gnai1* (Gi1), *Gnai2* (Gi2), *Gnai3* (Gi3), *Gnaq* (Gq), and *Gnas* (Gs) mRNAs. PCR using gene-specific primers was performed with cDNA generated from aVSMC and aorta tissue. Actin primers were used to monitor cDNA synthesis. Two to three independent experiments were performed and showed similar results.

GPCR signaling assay. VSMC from explanted thoracic aortic tissue were prepared as described previously (12). Cells were seeded onto poly-L-lysine (Sigma-Aldrich, St. Louis, MO)-coated glass chamber slides and stained with anti-smooth muscle-actin antibody (Sigma-Aldrich) and Hoechst 33324 DNA dye (Invitrogen, Carlsbad, CA), indicating that cell preparations were more than 80% VSMC. Cells in culture were maintained in Dulbecco's modified Eagle's medium-F12 containing 20% fetal calf serum and 2 mM glutamine with penicillin and streptomycin and were serum starved for 24 h prior to the signaling assays. Angiotensin II, endothelin-1 (ET-1), isoproterenol, sphingosine 1-phosphate (S1P), and sodium nitroprusside (SNP) were purchased from Sigma-Aldrich. Anti-phospho-extracellular signal-regulated kinase (anti-phospho-ERK) and antibodies to phospho-vasodilator-stimulated protein (phospho-VASP; phosphorylated at Ser157 or Ser239) were purchased from Cell Signaling Technology Inc. (Danvers, MA), and antiactin antibody was purchased from Santa Cruz Biotechnology Inc. (Santa Cruz, CA).

RESULTS

Generation of $Rgs5^{-/-}$ mutant mice. Located on mouse chromosome 1, *Rgs5* spans approximately 40 kb and contains five exons, of which the last three contribute to the encoding of the RGS domain. For the generation of a targeting construct, a 16-kb mouse genomic DNA fragment containing the *Rgs5* gene was isolated from a mouse 129Sv/Ev lambda genomic library. An 8.5-kb fragment with exon 1 was subcloned from the genomic fragment, and a dual cassette of *lacZ* and neomycin resistance genes was inserted between the point 7 bp upstream of the ATG start codon in exon 1 and the point 2,560 bp downstream of exon 1, deleting parts of exon 1 and intron

1 (Fig. 1A). After the screening of embryonic stem cell clones, one targeted embryonic stem cell clone was used to establish chimeric mice, which were crossed with C57BL/6 mice to obtain *Rgs5* heterozygotes. All mice analyzed were obtained from intercrosses of the *Rgs5* heterozygotes. PCR primers designed to amplify products of different sizes from the wild-type and the mutated alleles gave bands of the predicted sizes (Fig. 1B).

RT-PCR analysis of RNAs prepared from aorta tissue and cultured aortic VSMC (aVSMC) demonstrated the presence and absence of *Rgs5* mRNA in control and *Rgs5*-targeted mice, respectively (Fig. 1C). Compensatory changes in the expression of certain G proteins were observed when a G protein gene was targeted or silenced, revealing the adaptability of G protein signaling networks (10, 17). We therefore tested whether the lack of RGS5 induced any changes in the expression of various RGS or G_{α} mRNAs by using RT-PCR (Fig. 1C). Interestingly, levels of RGS16 mRNA in RGS5-deficient aorta tissue and aVSMC were considerably higher than those in wild-type samples. A modest increase in the level of a member of the $G_{i\alpha}$ subfamily, $G_{i\alpha 3}$, in RGS-deficient aorta tissue compared to that in wild-type aorta tissue was observed. Although DNA sequence analysis of genomic DNA of *Rgs5*$^{-/-}$ mice showed appropriate cloning and targeting, we failed to detect β-galactosidase activity from tissues tested, suggesting that transcriptional and/or translational elements in the deleted region are necessary for *Rgs5* expression in vivo. Previously, when the *Rgs5* gene was mutated in mice by the insertion of a vector containing the *lacZ* gene, a very high level of β-galactosidase expression in blood vessels was detected (http://www.informatics.jax.org/external/ko/deltagen/459.html). Strong punctuate staining of β-galactosidase was observed in the outer layers of vessels, but not in the innermost endothelial layer, a result consistent with previous findings (1, 7).

Phenotypic analysis of *Rgs5*$^{-/-}$ mutant mice. RGS5-deficient mice did not exhibit any gross abnormalities but were leaner than littermate control mice. In general, there were no significant differences detected in the heterozygous or homozygous mutant animals compared with age- and gender-matched wild-type control mice. Mice homozygous for the *Rgs5* mutation exhibited no difficulties in breeding and no obvious gross abnormalities. The comparison of organ and body weights of *Rgs5*$^{+/+}$ and *Rgs5*$^{-/-}$ mice by using single-factor analysis of variance failed to reveal any significant differences in heart, liver, brain, kidney, thymus, or spleen weights (data not shown). Extensive hematology, serum chemistry analysis, and histopathology examination of six 2-month-old mice of each genotype revealed no apparent abnormalities (data not shown). A statistically significant difference in the absolute counts of blood lymphocytes was found. The mean value for six *Rgs5*$^{-/-}$ mice was $1.32 \times 10^3 \pm 0.12 \times 10^3$/ml, compared to $2.81 \times 10^3 \pm 0.529 \times 10^3$/ml for littermate control mice ($P = 0.0008$). The significance of this difference was unclear, since all values were within the normal range as defined by the Division of Veterinary Resources, Office of Research Services, National Institutes of Health (0.36×10^3 to 4.46×10^3/ml). Since RGS5 mRNA expression in lymphocytes was not observed (data not shown), the reduced blood lymphocyte counts may be the result of altered lymphocyte trafficking, such as increased ingress to or inefficient egress from lymphoid organs.

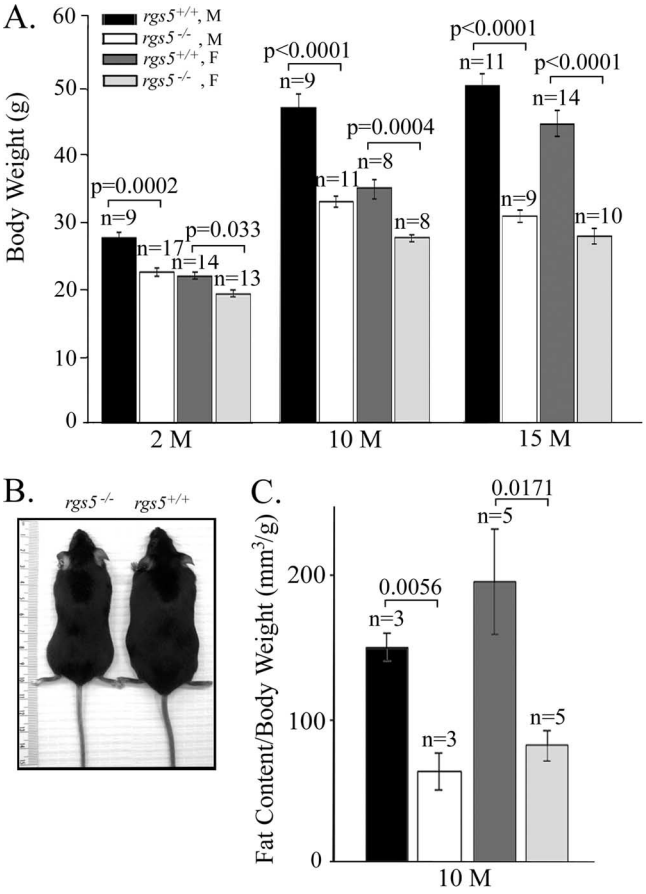

FIG. 2. RGS5-deficient mice are lean. (A) Body weights of male (M) and female (F) *Rgs5*$^{+/+}$ and *Rgs5*$^{-/-}$ mice were measured at 2 (2 M), 10 (10 M), and 15 (15 M) months. The numbers of animals (*n*) used are shown. Data shown are the means ± standard errors of the means (SEM). Both male and female homozygous mice had significantly reduced body weights compared to those of age-matched littermate controls. (B) Female *Rgs5*$^{+/+}$ and *Rgs5*$^{-/-}$ mice aged 7 and 1/2 months old were photographed. (C) CT was performed with 10-month-old mice injected with Fenestra-VC. Relative fat contents were obtained by the analysis of reconstructed three-dimensional images using Amira 4.1. The numbers of animals used are shown. Data shown are the means ± SEM. Data were analyzed for statistical significance by Student's *t* test, and *P* values are indicated above the bars.

The expression of RGS5 in the conduits of lymphoid organs is currently being examined.

All mice were fed normal chow, and their weights were measured at 2, 10, and 15 months of age. Male and female *Rgs5*$^{-/-}$ mice weighed less than littermate controls at all time points, and the weight difference became more apparent as the animals aged (Fig. 2A and B). This finding is contradictory to the results in a previous study reporting that there was no statistically significant difference in body weight between wild-type and RGS5-deficient mice (http://www.informatics.jax.org/external/ko/deltagen/459.html). The contradiction is probably due to the difference in the mouse strains used. The levels of cholesterol and triglycerides and nonfasting glucose levels in six 2-month-old mice of each genotype fell within normal ranges (data not shown). The relative fat contents per gram of weight of the littermate controls were significantly higher

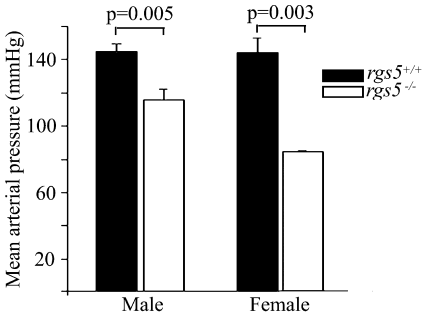

FIG. 3. RGS5-deficient mice are hypotensive. Three-day means of arterial pressure measurements for $Rgs5^{+/+}$ and $Rgs5^{-/-}$ mice are shown. For each genotype, five male and three female mice were used. Mice were acclimated to the BP machine for 2 days, and the actual BPs were measured 20 times consecutively after 10 cycles of mock measurement for 3 days. Acclimation and measurement were performed in the morning with nonanesthetized mice. Data shown are the means ± SEM. Data were analyzed for statistical significance by Student's *t* test.

than those of the $Rgs5^{-/-}$ mice when measured by CT at the age of 10 months (Fig. 2C). RGS5 was previously reported to be expressed in mouse adipocytes isolated from subcutaneous and intra-abdominal fat (http://www.ncbi.nlm.nih.gov/projects/geo/gds/profileGraph.cgi?&dataset=zb5LIV9doGAR&dataset=d76WU19acSJ_$&gmin=47.271200&gmax=1014.820000&absc=210986p1p1p1p1p1&gds=2818&idref=103294_at&annot=Rgs5). In a previous study, the levels of *Rgs5* mRNA in the inguinal adipose tissue of C57BL/6J males were higher in high weight gainers than in low weight gainers after 4 weeks on a high-saturated-fat diet (http://www.ncbi.nlm.nih.gov/projects/geo/gds/profileGraph.cgi?&dataset=AYGzxl&dataset=mpnsrq$&gmin=48681.000000&gmax=96279.000000&absc=&gds=2319&idref=401103&annot=Rgs5). Interestingly, in another previous study, knock-in mice expressing RGS-insensitive $G_{i\alpha 2}$ also exhibited lower body weights and smaller fat stores than control mice (14). However, the phenotype was significantly blunted after backcrossing into another mouse strain (14). Together, these results demonstrate critical roles of RGS proteins and $G_{i\alpha 2}$ in the control of body weight and metabolism, although their impact is modulated by the genetic background of the mice.

RGS5-deficient mice exhibit low BP without concomitant cardiac dysfunction. To assess whether RGS5 was required for normal BP homeostasis, we measured the tail BPs of awake wild-type and $Rgs5^{-/-}$ mice. The lack of RGS5 caused hypotension, and the reduction in BP differed by sex, with females having lower levels than male mice (Fig. 3). The average mean arterial pressure for five male $Rgs5^{-/-}$ mice was 116 ± 6 mm Hg, which was significantly lower than the 145 ± 5 mm Hg for wild-type littermate controls ($P = 0.005$). The average mean arterial pressure for three female $Rgs5^{-/-}$ mice was 84 ± 1 mm Hg, compared with 144 ± 9 mm Hg for wild-type littermate controls ($P = 0.003$). The tail cuff BP analysis system was not suitable for studies to pharmacologically modify BP. Transthoracic echocardiography analyses of anesthetized mice by using a microultrasound system revealed that relative to wild-type littermates, RGS5-deficient mice exhibited neither a significant decrease in systolic contractile function, as measured by the percentage of fractional shortening and the ejection fraction, nor evidence of hyper- or hypotrophy, as indicated by various cardiac dimensions (Table 1). Further examination of the cardiac rhythms of conscious mice by electrocardiography revealed no statistically significant difference between RGS5-deficient mice and control mice (Table 2). RGS5-deficient and control mice had similar heart rates whether awake or under anesthesia.

Analysis of blood vessels from the RGS5-deficient mice reveals increased aorta diameters. Based on the strong expression of *Rgs5* in developing blood vessels and persistent expression in the aortas of adult mice, it was of interest to perform histology and morphometric analyses of vasculature such as aorta and kidney resistance arteries for any abnormalities. The aortas from four mice of each genotype were excised at the same places by using body landmarks. Three sections from each mouse, the ascending aorta, the midthoracic area, and the area just proximal to the diaphragm, were prepared. Inner and outer circumferences and medial thicknesses of these aorta sections were measured and averaged for comparison (Fig. 4A to C). Both the inner and outer circumferences of the sections from the RGS5-deficient mice were significantly larger than those of the sections from littermates. No alteration in the medial thickness indicative of VSMC hypo- or hypertrophy was

TABLE 1. Echocardiographic analysis of wild-type and RGS5-deficient mice[a]

Measurement	Value for male $Rgs5^{+/+}$ mice ($n = 4$)	Value for male $Rgs^{-/-}$ mice ($n = 3$)	Value for female $Rgs5^{+/+}$ mice ($n = 4$)	Value for female $Rgs^{-/-}$ mice ($n = 4$)
Cardiac dimensions				
LVPWd (mm)	0.92 ± 0.09	0.89 ± 0.09	0.77 ± 0.03	0.79 ± 0.04
IVSd (mm)	0.78 ± 0.02	0.87 ± 0.02	0.81 ± 0.07	0.79 ± 0.08
LVIDd (mm)	4.20 ± 0.21	4.03 ± 0.18	3.83 ± 0.10	3.64 ± 0.06
LVPWs (mm)	1.27 ± 0.09	1.13 ± 0.18	1.07 ± 0.13	1.20 ± 0.05
IVSs (mm)	1.28 ± 0.10	1.33 ± 0.07	1.19 ± 0.08	1.11 ± 0.04
LVIDs (mm)	2.64 ± 0.11	2.72 ± 0.22	2.67 ± 0.17	2.33 ± 0.12
Fractional shortening (%)	37.2 ± 1.2	32.9 ± 5.6	32.1 ± 2.7	38.7 ± 1.3
Ejection fraction (%)	67.5 ± 1.3	60.9 ± 7.7	61.0 ± 3.6	69.7 ± 1.5
Heart rate (bpm)	418 ± 15	424 ± 9	436 ± 22	448 ± 39

[a] Echocardiography was performed with anesthetized mice by using the VisualSonics microultrasound system. Abbreviations: LVPWd, left ventricle posterior wall, diastolic; IVSd, interventricular septum, diastolic; LVIDd, left ventricle internal dimension, diastolic; LVPWs, left ventricle posterior wall, systolic; IVSs, interventricular septum, systolic; LVIDs, left ventricle internal dimension, systolic; and bpm, beats per minute. The fractional shortening and ejection fraction values were obtained using VisualSonics software. Data shown are the means ± SEM.

TABLE 2. Electrocardiographic analysis of wild-type and RGS5-deficient mice[a]

Measurement	Value for male $Rgs5^{+/+}$ mice ($n = 5$)	Value for male $Rgs^{-/-}$ mice ($n = 5$)	Value for female $Rgs5^{+/+}$ mice ($n = 3$)	Value for female $Rgs^{-/-}$ mice ($n = 3$)
Heart rate (bpm)	653 ± 30	706 ± 17	695 ± 24	673 ± 24
P-R interval (ms)	32 ± 1.4	30.0 ± 0.9	27.8 ± 2.0	31.4 ± 1.4
Duration of QRS complex (ms)	12.3 ± 0.3	12.1 ± 0.6	12.2 ± 0.4	11.6 ± 0.3
Q-T interval (ms)	45.3 ± 1.3	43.4 ± 1.2	42.3 ± 1.4	44.0 ± 1.7

[a] Electrocardiography was performed with conscious mice by using ECGenie. Data shown are the means ± SEM. bpm, beats per minute.

found, although a slight increase in the ratio between the thickest and thinnest portions of the aorta walls in the RGS5-deficient mice was noted.

To assess the renovasculature, 20 kidney resistance vessels with diameters of 50 to 100 μm from each genotype were analyzed. In contrast to observations with the RGS2-deficient mice, no statistically significant change in the thickness of these arteries in RGS5-deficient mice that would suggest VSMC hypertrophy and/or hyperproliferation was found (Fig. 4D and E). Since it was not feasible to map the exact location of renal

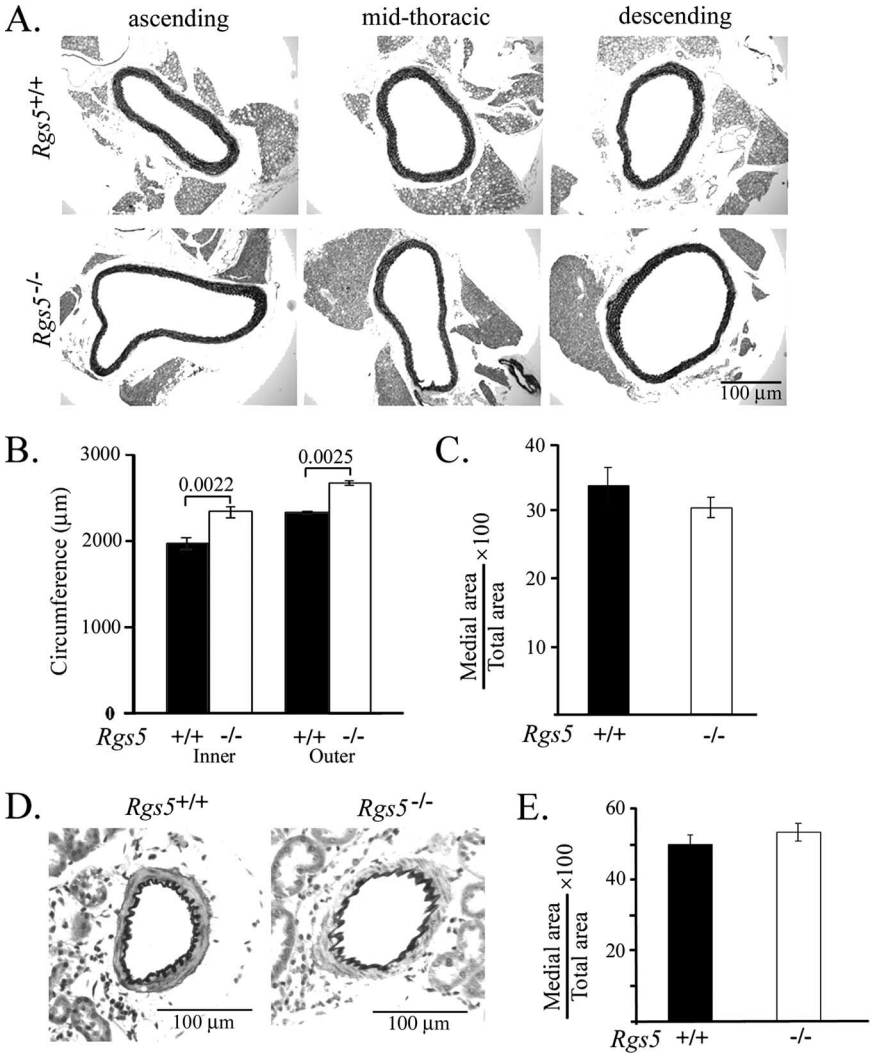

FIG. 4. The aortas in RGS5-deficient mice are dilated. (A) Representative images of VGE-stained aorta sections from $Rgs5^{+/+}$ and $Rgs5^{-/-}$ mice are shown. Aortas were harvested from four mice of each genotype, and sections were made from three areas: ascending (proximal to the heart), midthoracic, and descending (proximal to the diaphragm). (B and C) Morphometric analysis of aortas. The mean inner and outer circumferences (B) and mean relative medial thicknesses (medial area/total area × 100) (C) of sections from four mice of each genotype are shown. Numbers above the bars in panel B are *P* values. (D) Representative images of VGE-stained kidney resistance vessels (diameters of 50 to 100 μm) from $Rgs5^{+/+}$ and $Rgs5^{-/-}$ mice. (E) Morphometric analysis of the renovasculature. The mean relative medial thicknesses of approximately 20 kidney resistance vessels from each genotype are shown. Data are the means ± SEM. Data were analyzed for statistical significance by Student's *t* test. Images were captured with Image-Pro, and data were obtained by using the measurement module of Image-Pro.

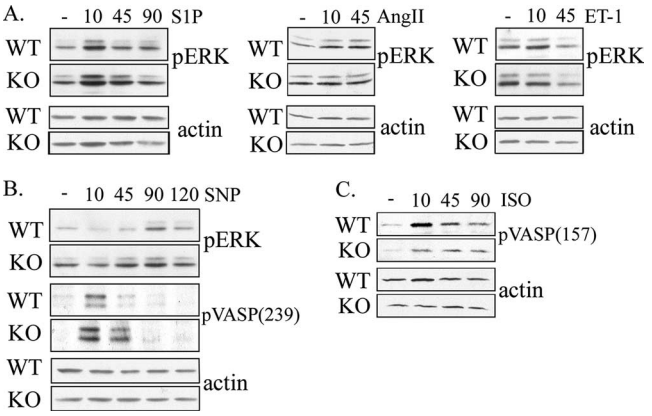

FIG. 5. Signaling assays. Aortic smooth muscle cells were isolated from *Rgs5*$^{+/+}$ and *Rgs5*$^{-/-}$ mice and cultured in Dulbecco's modified Eagle's medium-F12 containing 20% fetal calf serum. Cells were serum starved for 24 h and treated with angiotensin II (AngII; 1 μM), ET-1 (100 nM), isoproterenol (ISO; 10 μM), S1P (100 nM), or SNP (1.5 mM) for the times indicated (in minutes). Cells were then lysed in a lysis buffer and used for Western blot analysis with anti-phospho-ERK antibody (pERK) and antibodies to phospho-VASP phosphorylated at Ser157 [pVASP(157)] and Ser239 [pVASP(239)]. The same protein membranes were immunoblotted with antiactin antibody for the normalization of protein loading. Two to five independent experiments were performed and showed similar results. WT, wild type; KO, knockout; −, unstimulated.

vessels using body landmarks, we did not attempt to measure the circumferences of the kidney vessels. Computerized tomography performed after the injection of the contrast agent Fenestra VC revealed no apparent anatomical malformations of the blood vessels (data not shown).

Altered signaling in aVSMC prepared from RGS5-deficient mice. Next, we cultured VSMC from the excised aortas of wild-type and RGS5-deficient mice to examine whether the loss of RGS5 caused any altered signaling events relevant to the hypotensive phenotype (Fig. 5). Since the overexpression of RGS5 is known to impair angiotensin II-, ET-1-, and S1P-induced ERK phosphorylation and RGS5 protein stability is likely to be under the control of the nitric oxide (NO)-mediated N-end rule pathway, we tested whether RGS5-deficient VSMC responded differently than wild-type cells to these GPCR ligands or SNP, an NO donor. The phosphorylation of ERK in response to S1P was clearly enhanced in RGS5-deficient aVSMC compared to that in wild-type aVSMC (Fig. 5A). In contrast, the lack of RGS5 did not cause any changes in angiotensin II- or ET-1-induced ERK phosphorylation. RT-PCR analysis with RNAs isolated from aVSMC and aorta tissue did not show any difference in levels of mRNA for $S1P_1$ to $S1P_5$ receptors between wild-type and RGS5-deficient mice (data not shown). Despite serum starvation prior to signaling assays, the level of ERK phosphorylation in nonstimulated RGS5-deficient aVSMC was always higher than that in wild-type aVSMC. This finding suggests a prolonged and aberrant response of RGS5-deficient aVSMC to stimuli present in serum. This effect may blunt the angiotensin II- or ET-1-induced ERK phosphorylation in RGS5-deficient cells. Upon stimulation with SNP, higher levels of ERK and VASP Ser239 phosphorylation in RGS5-deficient aVSMC than in wild-type aVSMC were observed (Fig. 5B). Unexpectedly, RGS5-deficient cells showed dysregulated kinetics of VASP Ser157 phosphorylation in response to isoproterenol (Fig. 5C). Ser239 and Ser157 of VASP are the major protein kinase G and protein kinase A phosphorylation sites, respectively, and are used as the readout for vasodilation in VSMC (22, 25). Unlike ERK phosphorylation levels, the basal VASP phosphorylation levels in nonstimulated RGS5-deficient aVSMC remained low, as those in wild-type aVSMC. In general, we did not observe any differences between male and female mice in the signaling pathways examined (data not shown).

DISCUSSION

The potent GAP activity of RGS5 toward $G_{i\alpha}$ and $G_{q\alpha}$ and its striking expression pattern in blood vessels suggested a fundamental role in blood vessel development and/or physiology (1, 5, 7). The demonstration of the dynamic regulation of *Rgs5* in numerous previous studies further supports the potential significance of RGS5 in tumor angiogenesis, atherosclerosis, and smooth-muscle-cell pathology (2, 4, 19). Here, we focus on the role of RGS5 in BP regulation and report that, surprisingly, the *Rgs5*-targeted mice are hypotensive. It is also noteworthy that RGS5-deficient mice are significantly leaner than wild-type mice, especially as they age, which certainly warrants additional study. There was no significant difference in heart rate or in cardiac function between the control and *Rsg5*-targeted mice, suggesting that the decrease in BP seen in *Rgs5*$^{-/-}$ mice was not caused by impaired cardiac output. The increased diameters of the aortas in RGS5-deficient mice may have resulted from a developmental defect or aortic remodeling due to the chronic low BP. It is unlikely that changes in a conduit vessel such as the aorta per se contribute to the decreased BP noted in the *Rgs5*$^{-/-}$ mice. The difference between the BPs of the male and female *Rgs5*$^{-/-}$ mice does not represent the first gender difference in BPs. It has been noted in studies of GPCR-regulated signaling pathways involved in BP control, as the transgenic expression of GRK5 more severely affects male mice (15).

The release of paracrine vasodilators from endothelial cells is a critical determinant of vascular tone. Many of the endothelium-dependent agonists that trigger vasodilation do so by one of three mechanisms: increasing the release of NO, increasing the release of prostacyclin, or using an ill-defined factor or factors termed endothelium-derived hyperpolarizing factor. The confinement of *Rgs5* expression to vascular smooth muscle/pericytes argues that the lack of RGS5 should not affect the release of vasodilatory factors from the endothelium. Most of the effects of NO on vascular smooth muscle relaxation occur by the activation of soluble guanylyl cyclase and an increase in cyclic GMP (cGMP). In addition, NO has been reported to reduce $G_{i\alpha}$ protein expression and, thus, increase levels of cyclic AMP (cAMP) in VSMC (3). Prostacyclin signals through a $G_{s\alpha}$-coupled receptor to increase cAMP levels in VSMC (20, 21). The exact nature of endothelium-derived hyperpolarizing factor, the third vasodilatory factor, and the mechanism by which it triggers smooth-muscle relaxation remain controversial (for a review, see reference 16). In general, $G_{i\alpha}$ and $G_{q\alpha}$ signaling pathways in VSMC are linked to elevating BP rather than reducing it. The β2-adrenergic receptor, another vasorelax-

ation GPCR in VSMC, also signals via $G_{\alpha s}$. Based on the known function of RGS5 as a $G_{i\alpha}$ and $G_{q\alpha}$ GAP, the loss of RGS5 from VSMC would not be predicted to alter cGMP- or cAMP-mediated signaling. Yet enhanced VASP Ser239 phosphorylation in response to SNP and aberrant kinetics of VASP Ser157 phosphorylation induced by isoproterenol were observed in *Rgs5*$^{-/-}$ aVSMC. The mechanism by which the loss of RGS5 may modify these signaling pathways is currently unknown. Unlike RGS2, which directly interferes with the activation of certain isoforms of adenylyl cyclase, RGS5 does not affect the activation of adenylyl cyclases in purified olfactory epithelia (27). The reduced responsiveness to isoproterenol in *Rgs5*$^{-/-}$ aVSMC may be the consequence of chronic vasorelaxation. We cannot completely exclude the possibility that altered signaling in RGS5-deficient mice may be due to compensatory changes in vivo and the readjustment of cells in culture. The effect of enhanced S1P signaling in *Rgs5*$^{-/-}$ aVSMC remains unclear, since there are contradictory findings of both vasoconstriction and vasorelaxation responses to S1P, and despite numerous studies, a clear understanding of the role of S1P in regulating vascular tone remains elusive (for a review, see reference 23).

Among 30 or so RGS family members, RGS4, RGS5, and RGS16 contain an N-terminal cysteine motif that promotes arginyl transferase-mediated protein degradation via the N-end rule pathway (13, 18). The oxidation of N-terminal Cys is essential for its arginylation, and the oxidation requires NO prior to arginylation, implying that the stability of these proteins is likely under the control of NO. This implication suggests that RGS5 may attenuate vasodilation signaling. The compensatory increase in the level of mRNA for RGS16, which is also under the control of the N-end rule pathway, suggests that RGS16 may also act as a negative regulator for vasodilation signaling. More severe reduction in BP may have been observed without the increased RGS16 mRNA. In contrast, NO/cGMP-activated protein kinase GI-α phosphorylates RGS2, enhancing its GAP activity, and promotes the membrane localization of RGS2 (28, 29). This leads to the attenuation of vasoconstrictor GPCR signaling. NO may communicate with GPCR signaling pathways to relax vessels via two independent mechanisms. NO may inhibit GPCR-mediated vasoconstriction by increasing the GAP activity of RGS2 via phosphorylation and promoting the membrane recruitment of RGS2. NO may further increase vasorelaxation by promoting the degradation of RGS5 and/or RGS16, inhibitors of vasodilation signaling. This possibility is consistent with the observation that the lack of RGS2 causes hypertension but that the lack of RGS5 induces hypotension. The receptor selectivity of these RGS proteins may account for this difference. The lack of RGS2, but not RGS5, enhances vasoconstriction signaling/vasoreactivity mediated by GPCRs such as angiontensin II and ET-1 (11, 26).

In conclusion, the results of this and previous studies underscore the significance of fine-tuning GPCR signaling pathways via the regulation of the activity and expression of certain RGS proteins for maintaining normal BP. Further insight from dissecting the underlying mechanism of hypotension may provide novel strategies to treat hypertension.

ACKNOWLEDGMENTS

We thank members of the NIH Mouse Imaging Facility and Brenda Klaunberg and Martin Lizak for their helpful discussion and technical support. We also thank Anthony Fauci for his continuing support and Mary Rust for editorial assistance.

This work is supported by the intramural research program of NIAID, NIH.

REFERENCES

1. **Adams, L. D., R. L. Geary, B. McManus, and S. M. Schwartz.** 2000. A comparison of aorta and vena cava medial message expression by cDNA array analysis identifies a set of 68 consistently differentially expressed genes, all in aortic media. Circ. Res. **87:**623–631.
2. **Adams, L. D., R. L. Geary, J. Li, A. Rossini, and S. M. Schwartz.** 2006. Expression profiling identifies smooth muscle cell diversity within human intima and plaque fibrous cap: loss of RGS5 distinguishes the cap. Arterioscler. Thromb. Vasc. Biol. **26:**319–325.
3. **Bassil, M., and M. B. Anand-Srivastava.** 2006. Nitric oxide modulates Gi-protein expression and adenylyl cyclase signaling in vascular smooth muscle cells. Free Radic. Biol. Med. **41:**1162–1173.
4. **Berger, M., G. Bergers, B. Arnold, G. J. Hammerling, and R. Ganss.** 2005. Regulator of G-protein signaling-5 induction in pericytes coincides with active vessel remodeling during neovascularization. Blood **105:**1094–1101.
5. **Bondjers, C., M. Kalen, M. Hellstrom, S. J. Scheidl, A. Abramsson, O. Renner, P. Lindahl, H. Cho, J. Kehrl, and C. Betsholtz.** 2003. Transcription profiling of platelet-derived growth factor-B-deficient mouse embryos identifies RGS5 as a novel marker for pericytes and vascular smooth muscle cells. Am. J. Pathol. **162:**721–729.
6. **Chang, Y. P., X. Liu, J. D. O. Kim, M. A. Ikeda, M. R. Layton, A. B. Weder, R. S. Cooper, S. L. R. Kardia, D. C. Rao, S. C. Hunt, A. Luke, E. Boerwinkle, and A. Chakravarti.** 2007. Multiple genes for essential-hypertension susceptibility on chromosome 1q. Am. J. Hum. Genet. **80:**253–264.
7. **Cho, H., T. Kozasa, C. Bondjers, C. Betsholtz, and J. H. Kehrl.** 2003. Pericyte-specific expression of Rgs5: implications for PDGF and EDG receptor signaling during vascular maturation. FASEB J. **17:**440–442.
8. **Eckhart, A. D., T. Ozaki, H. Tevaearai, H. A. Rockman, and W. J. Koch.** 2002. Vascular-targeted overexpression of G protein-coupled receptor kinase-2 in transgenic mice attenuates beta-adrenergic receptor signaling and increases resting blood pressure. Mol. Pharmacol. **61:**749–758.
9. **Felder, R. A., and P. A. Jose.** 2006. Mechanisms of disease: the role of GRK4 in the etiology of essential hypertension and salt sensitivity. Nat. Clin. Pract. Nephrol. **2:**637–650.
10. **Han, S. B., J. Y. Song, Y. S. Yun, S. Y. Yi, C. Moratz, N. N. Huang, B. Kelsall, H. Cho, C. S. Shi, O. Schwartz, and J. H. Kehrl.** 2005. Rgs1 and Gnai2 regulate the entrance of B lymphocytes into lymph nodes and B cell motility within lymph node follicles. Immunity **22:**343–354.
11. **Hercule, H. C., J. Tank, R. Plehm, M. Wellner, A. C. da Costa Goncalves, M. Gollasch, A. Diedrich, J. Jordan, F. C. Luft, and V. Gross.** 2007. Regulation of G protein signalling 2 ameliorates angiotensin II-induced hypertension in mice. Exp. Physiol. **92:**1014–1022.
12. **Heximer, S. P., R. H. Knutsen, X. Sun, K. M. Kaltenbronn, M. H. Rhee, N. Peng, A. Oliveira-dos-Santos, J. M. Penninger, A. J. Muslin, T. H. Steinberg, J. M. Wyss, R. P. Mecham, and K. J. Blumer.** 2003. Hypertension and prolonged vasoconstrictor signaling in RGS2-deficient mice. J. Clin. Investig. **111:**445–452.
13. **Hu, R. G., J. Sheng, X. Qi, Z. Xu, T. T. Takahashi, and A. Varshavsky.** 2005. The N-end rule pathway as a nitric oxide sensor controlling the levels of multiple regulators. Nature **437:**981–986.
14. **Huang, X., R. A. Charbeneau, Y. Fu, K. Kaur, I. Gerin, O. A. MacDougald, and R. R. Neubig.** 2008. Resistance to diet-induced obesity and improved insulin sensitivity in mice with a regulator of G protein signaling-insensitive G184S Gnai2 allele. Diabetes **57:**77–85.
15. **Keys, J. R., R. H. Zhou, D. M. Harris, C. A. Druckman, and A. D. Eckhart.** 2005. Vascular smooth muscle overexpression of G protein-coupled receptor kinase 5 elevates blood pressure, which segregates with sex and is dependent on Gi-mediated signaling. Circulation **112:**1145–1153.
16. **Kohler, R., and J. Hoyer.** 2007. The endothelium-derived hyperpolarizing factor: insights from genetic animal models. Kidney Int. **72:**145–150.
17. **Krumins, A. M., and A. G. Gilman.** 2006. Targeted knockdown of G protein subunits selectively prevents receptor-mediated modulation of effectors and reveals complex changes in non-targeted signaling proteins. J. Biol. Chem. **281:**10250–10262.
18. **Lee, M. J., T. Tasaki, K. Moroi, J. Y. An, S. Kimura, I. V. Davydov, and Y. T. Kwon.** 2005. RGS4 and RGS5 are in vivo substrates of the N-end rule pathway. Proc. Natl. Acad. Sci. USA **102:**15030–15035.
19. **Li, J., L. D. Adams, X. Wang, L. Pabon, S. Schwartz, D. Sane, and R. Geary.** 2004. Regulator of G protein signaling 5 marks peripheral arterial smooth muscle cells and is downregulated in atherosclerotic plaque. J. Vasc. Surg. **40:**519–528.
20. **Meyer-Kirchrath, J., S. Debey, C. Glandorff, L. Kirchrath, and K. Schrör.**

2004. Gene expression profile of the Gs-coupled prostacyclin receptor in human vascular smooth muscle cells. Biochem. Pharmacol. **67:**757–765.

21. **Nobles, M., A. Benians, and A. Tinker.** 2005. Heterotrimeric G proteins precouple with G protein-coupled receptors in living cells. Proc. Natl. Acad. Sci. USA **102:**18706–18711.
22. **Oelze, M., H. Mollnau, N. Hoffmann, A. Warnholtz, M. Bodenschatz, A. Smolenski, U. Walter, M. Skatchkov, T. Meinertz, and T. Münzel.** 2000. Vasodilator-stimulated phosphoprotein serine 239 phosphorylation as a sensitive monitor of defective nitric oxide/cGMP signaling and endothelial dysfunction. Circ. Res. **87:**999–1005.
23. **Peters, S. L., and A. E. Alewijnse.** 2007. Sphingosine-1-phosphate signaling in the cardiovascular system. Curr. Opin. Pharmacol. **7:**186–192.
24. **Rosskopf, D., M. Schurks, C. Rimmbach, and R. Schafers.** 2007. Genetics of arterial hypertension and hypotension. Naunyn-Schmiedeberg's Arch. Pharmacol. **374:**429–469.
25. **Schafer, A., M. Burkhardt, T. Vollkommer, J. Bauersachs, T. Munzel, U. Walter, and A. Smolenski.** 2003. Endothelium-dependent and -independent relaxation and VASP serines 157/239 phosphorylation by cyclic nucleotide-elevating vasodilators in rat aorta. Biochem. Pharmacol. **65:**397–405.
26. **Semplicini, A., L. Lenzini, M. Sartori, M., I. Papparella, L. A. Calo, E. Pagnin, G. Strapazzon, C. Benna, R. Costa, A. Avogaro, G. Ceolotto, and A. C. Pessina.** 2006. Reduced expression of regulator of G-protein signaling 2 (RGS2) in hypertensive patients increases calcium mobilization and ERK1/2 phosphorylation induced by angiotensin II. J. Hypertens. **24:**1115–1124.
27. **Sinnarajah, S., C. W. Dessauer, D. Srikumar, J. Chen, J. Yuen, S. Yilma, J. C. Dennis, E. E. Morrison, V. Vodyanoy, and J. H. Kehrl.** 2001. RGS2 regulates signal transduction in olfactory neurons by attenuating activation of adenylyl cyclase III. Nature **409:**1051–1055.
28. **Sun, X., K. M. Kaltenbronn, T. H. Steinberg, and K. J. Blumer.** 2005. RGS2 is a mediator of nitric oxide action on blood pressure and vasoconstrictor signaling. Mol. Pharmacol. **67:**631–639.
29. **Tang, K. M., G. R. Wang, P. Lu, R. H. Karas, M. Aronovitz, S. P. Heximer, K. M. Kaltenbronn, K. J. Blumer, D. P. Siderovski, Y. Zhu, and M. E. Mendelsohn.** 2003. Regulator of G-protein signaling-2 mediates vascular smooth muscle relaxation and blood pressure. Nat. Med. **9:**1506–1512.